

Observation of Hexagonal Close-Packed Water Ice at Extreme Pressures and Temperatures

Alexis Forestier,^{1, 2,*} Gunnar Weck,^{1, 2} Sandra Ninet,³ Gaston Garbarino,⁴ Mohamed Mezouar,⁴ Frédéric Datchi,³ and Paul Loubeyre^{1, 2}

¹CEA DAM DIF, F-91297 Arpajon, France

²Université Paris-Saclay, CEA, Laboratoire Matière en Conditions Extrêmes, F-91680 Bruyères-le-Châtel, France

³Institut de Minéralogie, de Physique des Matériaux et de Cosmochimie (IMPMC), Sorbonne Université, CNRS UMR 7590, IRD UMR 206, MNHN, 4 place Jussieu, F-75005 Paris, France

⁴European Synchrotron Radiation Facility, Boîte Postale 220, F-38043 Grenoble, France

The determination of the phase diagram of water ice under extreme conditions remains a fundamental challenge in high-pressure physics. While theoretical predictions have long suggested the existence of compact phases, such as face-centered cubic (fcc) and hexagonal close-packed (hcp) structures, yet only the fcc phase has been experimentally confirmed. Here, we report the first direct observation of a hcp ice phase using synchrotron x-ray diffraction in laser-heated diamond anvil cells. Between 80 and 200 GPa, we observe the coexistence of fcc and hcp ice, arising from stacking disorder in the fcc oxygen layers, similar to phenomena seen in compressed noble gases. Above 200 GPa, the hcp phase becomes dominant and is recovered at 300 K, indicating its increased thermodynamic stability at ultrahigh pressures. These findings not only expand our understanding of water's complex behavior under extreme conditions but also may play a crucial role in the interiors of giant icy planets.

Exploring the phase diagram of water ice has continuously driven leading-edge experimental developments over the past century [1]. Water ice exhibits rich polymorphism owing to its hydrogen-bonding capability, which persists up to the tens-of-gigapascal range. A symmetric phase, ice X—considered an ionic solid—exists above approximately 50 GPa [2], featuring a body-centered cubic (bcc) oxygen sublattice. Today, the phase diagram of H₂O is being explored in the multi-megabar range and at high temperatures, using both static and dynamic experimental techniques [3–7], due to its fundamental importance and planetary implications.

Several theoretical calculations have predicted compact structures beyond bcc ice X—either (i) through further compression at ambient temperature into the multi-megabar regime [8–10], or (ii) within the ~ 100 GPa range combined with elevated temperatures [11–13]. These compact ices differ essentially regarding the stacking sequence of the close-packed oxygen layers. They either adopt a face-centered cubic (fcc), or an hexagonal close-packed (hcp) configuration or slightly distorted variants, e.g. the *Pbcm* structure [8]. Advanced computational methods—enabling simulations of large systems over long time scales and incorporating nuclear quantum effects—show that the free energies of fcc and hcp (or quasi-hcp) arrangements are almost identical in a wide thermodynamic P-T range [12, 13]. Hence, the coexistence of fcc and hcp local arrangements has been predicted to emerge due to stacking disorder and/or plasticity [12–14].

The first experimental evidence for the fcc phase was obtained via multi-shock compression [4]. This phase,

now designated as ice XVIII, is predicted to be superionic with hydrogen ions diffusing rapidly within the fcc oxygen lattice, resulting in very high ionic conductivity. The fcc superionic phase was confirmed and further investigated by x-ray diffraction (XRD) in the laser-heated diamond anvil cell (DAC) [5, 6]. Finally, the implementation of advanced sample geometries provided better constraints on its stability domain and enabled a detailed characterization of the superionic behavior, revealed through an X-ray signature showing anomalous thermal expansion with a crossover jump between two regimes [7].

Up to now, none of the other predicted compact structures has been experimentally observed. Here, we report the unambiguous observation of a novel H₂O ice form adopting a hcp oxygen sublattice, using synchrotron XRD of samples in the laser-heated DAC. In the range ~ 100 –200 GPa, the hcp structure is observed in coexistence with fcc and arises from stacking disorder of the oxygen dense planes when lowering temperature. At the highest pressures reached, near 220 GPa, the hcp phase is the only H₂O phase present in the high temperature diffraction pattern, indicating its likely thermodynamic stability over the fcc phase beyond 200 GPa.

Figure 1(a) shows a sketch of the sample geometry designed to probe the ice state under very high pressures and elevated temperatures. Membrane DACs equipped with beveled Boehler-type anvils and rhodium gaskets were used to compress ice samples. Within the DAC cavity, H₂O was confined between two cup-shaped boron-doped diamond (BDD) laser absorbers, forming a micro-oven. As demonstrated in our previous work [7], this setup enables efficient two-sided indirect laser heating (using 1070 nm YLF lasers) of the ice sample, minimizing temperature gradients thanks to the enclosing geometry and the high thermal conductivity of BDD [15]. Further

* alexis.forestier@cea.fr

technical details are given in the Materials and Methods section.

The present results were obtained in two runs using different samples. In the first run, we obtained high-quality single crystals of fcc ice by heating the sample up to 2000 K at around 80 GPa. As the temperature was ramped down, diffraction images were collected to investigate the thermal evolution of the fcc single-crystal-like peaks. As shown in Fig. 1 b, below approximately 1400 K, these diffraction peaks became noticeably deformed, and a weak diffuse intensity developed, connecting the 200 and 111 fcc peaks.

Upon further cooling, well-defined diffraction peaks appeared along the diffuse streaks, which can be unambiguously indexed by a hcp lattice. This evolution indicates a progressive splitting of the 111 fcc reflection into the 100, 002, and 101 hcp reflections. At 1086 K, the transformation remains incomplete, with the coexistence of fcc, hcp, and bcc domains.

Consistent with this interpretation, the d -spacings corresponding to the 111 fcc and 002 hcp reflections closely match, indicating that the two structures mainly differ in the stacking order of the dense oxygen planes. The integrated diffractogram collected at ~ 82 GPa and ~ 1086 K is shown in the bottom panel of Fig. 1c, displaying the full set of Bragg reflections from the fcc lattice ($a_{\text{fcc}} = 3.381$ Å), together with additional peaks from the hexagonal lattice ($a_{\text{hex}} = 2.383$ Å, $c_{\text{hex}} = 3.882$ Å). The latter yields a $c_{\text{hex}}/a_{\text{hex}}$ ratio of 1.629, consistent with the formation of an hcp polytype derived from the parent fcc structure.

In the second run, the ice sample was brought to over 200 GPa. During an initial compression of up to about 160 GPa, several thermal annealing cycles below 1500 K were performed to relieve non-hydrostatic stresses while keeping the sample within the stability field of bcc ice X and below its melting point. As expected, no additional diffraction features corresponding to other ice polymorphs were observed at this stage. Upon subsequent heating to higher temperatures (1800–2300 K) above 160 GPa, new diffraction peaks appeared, consistent with a coexistence of the hcp and fcc structures. Further compression to 197 GPa and heating to 2250 K led to an enhancement of the hcp reflections over the fcc ones (Fig. 1c, middle). Finally, after repeated heating cycles at 219 GPa up to 2630 K, the fcc peaks vanished and the hcp reflections became the sole observable phase (Fig. 1c, top).

As in run 1, the d -spacings of the 111 fcc and 002 hcp reflections coincide in the XRD patterns at 197 GPa. Inspection of the x-ray diffraction image corresponding to the 197 GPa pattern also revealed anomalous diffuse scattering streaks, showing the coexistence of fcc and hcp domains in the ice crystals due to stacking disorder. This observation resembles the case of compressed noble-gases, in which hcp and fcc polymorphs coexist through martensitic mechanisms across a broad thermodynamic P-T range [16–19].

In the present study and in refs (5, 7), the fcc phase was most frequently observed up to about 200 GPa, indicating its higher stability over a wide pressure range. However, we show here that fcc and hcp may coexist from approximately 80 to 200 GPa. Given their close enthalpies [12], coexistence of fcc and hcp domains over a broad pressure interval is plausible. The diffraction patterns further reveal a progressive evolution with pressure. At 82 GPa, the hcp reflections only appear upon cooling near 1086 K, when ice is transitioning from fcc to ice X. In contrast, at 197 GPa, both fcc and hcp reflections are simultaneously observed over a wide temperature range. Finally, at 219 GPa (Fig. 1c, top), the hcp peaks clearly dominate, suggesting that its relative stability increases beyond 200 GPa and eventually surpasses that of fcc. Furthermore, both fcc below 200 GPa [7] and hcp above could be recovered to ambient temperature, implying that their free energies remain competitive with that of ice X. This finding tends to contradict recent DFT-PBE calculations predicting that the bcc ice X is the most stable phase up to 300 GPa [13].

In conclusion, we report experimental evidence for another dense form of ice in which the oxygen atoms adopt an hcp lattice. This phase initially appears as stacking-disordered domains within the stable fcc phase, more likely through a martensitic mechanism. Above 200 GPa, hcp ice is systematically produced at high temperature and is the sole observed phase at 219 GPa, suggesting it becomes more stable than fcc ice. Further experimental work is required to precisely determine the respective P-T domains of stability of hcp, fcc and bcc ices. Another open question is whether hcp ice exists in a superionic state, which is an important issue for models of giant icy planets. The latter could be probed through measurements of its thermal expansion properties, as recently done for the fcc phase [7].

MATERIALS AND METHODS

Beveled Bohler-type diamond anvils with culet sizes of 150 μm and 50 μm were used for runs 1 and 2, respectively. Diamond anvils were FIB-machined to create two circular pits on the culet, designed to accommodate and stabilize the two BDD laser absorbers. The BDD absorbers were machined by femtosecond UV laser, and then finalized with focused ion beam (FIB) milling to achieve the desired geometry. Thermal insulation was ensured by a ~ 2.5 μm -thick Al_2O_3 coating applied to both anvils. In-situ XRD measurements were performed at the ID27 beamline of the European Synchrotron Radiation Facility (ESRF) [20]. The 0.3738 Å x-ray beam had a spot size of 0.6×0.6 μm^2 on the sample, ensuring high-quality XRD data despite the small sample size (~ 12 μm diameter at highest pressures of ~ 220 GPa). XRD images were collected on an Eiger2 X CdTe 9M detector (Dectris). The beamline uses a two-sided achromatic pyrometric system to determine temperature from the

BDD Planck thermal emission spectrum in the 550–930 nm range [20]. Sample pressure was evaluated from the volume of the BDD absorbers using the thermal equation of state of diamond given in ref. 21.

ACKNOWLEDGMENTS

We acknowledge the European Synchrotron Radiation Facility (ESRF) for provision of synchrotron beamtime under proposals number HC5078, and HC5699. The authors acknowledge the Agence Nationale de la Recherche (ANR) for financial support under Grant No. ANR-21-CE30-0032-01 (LILI).

[1] T. C. Hansen, The everlasting hunt for new ice phases, *Nature Communications* **12**, 3161 (2021).

[2] P. Loubeyre, R. LeToullec, E. Wolanin, M. Hanfland, and D. Hausermann, Modulated phases and proton centring in ice observed by X-ray diffraction up to 170 GPa, *Nature* **397**, 503 (1999).

[3] M. Millot, S. Hamel, J. R. Rygg, P. M. Celliers, G. W. Collins, F. Coppari, D. E. Fratanduono, R. Jeanloz, D. C. Swift, and J. H. Eggert, Experimental evidence for superionic water ice using shock compression, *Nature Physics* **14**, 297 (2018).

[4] M. Millot, F. Coppari, J. R. Rygg, A. Correa Barrios, S. Hamel, D. C. Swift, and J. H. Eggert, Nanosecond X-ray diffraction of shock-compressed superionic water ice, *Nature* **569**, 251 (2019).

[5] G. Weck, J.-A. Queyroux, S. Ninet, F. Datchi, M. Mezouar, and P. Loubeyre, Evidence and Stability Field of fcc Superionic Water Ice Using Static Compression, *Physical Review Letters* **128**, 165701 (2022).

[6] V. B. Prakapenka, N. Holtgrewe, S. S. Lobanov, and A. F. Goncharov, Structure and properties of two superionic ice phases, *Nature Physics* **17**, 1233 (2021).

[7] A. Forestier, G. Weck, F. Datchi, S. Ninet, G. Garbarino, M. Mezouar, and P. Loubeyre, X-Ray Signature of the Superionic Transition in Warm Dense fcc Water Ice, *Physical Review Letters* **134**, 076102 (2025), publisher: American Physical Society.

[8] M. Benoit, M. Bernasconi, P. Focher, and M. Parrinello, New High-Pressure Phase of Ice, *Physical Review Letters* **76**, 2934 (1996).

[9] B. Militzer and H. F. Wilson, New Phases of Water Ice Predicted at Megabar Pressures, *Physical Review Letters* **105**, 10.1103/PhysRevLett.105.195701 (2010).

[10] A. Hermann, N. W. Ashcroft, and R. Hoffmann, High pressure ices, *Proceedings of the National Academy of Sciences* **109**, 745 (2012).

[11] P. Demontis, R. LeSar, and M. L. Klein, New High-Pressure Phases of Ice, *Physical Review Letters* **60**, 2284 (1988).

[12] B. Cheng, M. Bethkenhagen, C. J. Pickard, and S. Hamel, Phase behaviours of superionic water at planetary conditions, *Nature Physics* **17**, 1228 (2021).

[13] A. Reinhardt, M. Bethkenhagen, F. Coppari, M. Millot, S. Hamel, and B. Cheng, Thermodynamics of high-pressure ice phases explored with atomistic simulations, *Nature Communications* **13**, 4707 (2022).

[14] F. Matusalem, J. Santos Rego, and M. de Koning, Plastic deformation of superionic water ices, *Proceedings of the National Academy of Sciences* **119**, e2203397119 (2022).

[15] G. Weck, V. Recoules, J.-A. Queyroux, F. Datchi, J. Bouchet, S. Ninet, G. Garbarino, M. Mezouar, and P. Loubeyre, Determination of the melting curve of gold up to 110 GPa, *Physical Review B* **101**, 014106 (2020).

[16] H. Cynn, C. S. Yoo, B. Baer, V. Iota-Herbei, A. K. McMahan, M. Nicol, and S. Carlson, Martensitic fcc-to-hcp Transformation Observed in Xenon at High Pressure, *Physical Review Letters* **86**, 4552 (2001).

[17] A. D. Rosa, A. Dewaele, G. Garbarino, V. Svitlyk, G. Morard, F. De Angelis, M. Krstulović, R. Briggs, T. Irifune, O. Mathon, and M. A. Bouhifd, Martensitic fcc-hcp transformation pathway in solid krypton and xenon and its effect on their equations of state, *Physical Review B* **105**, 144103 (2022).

[18] A. Dewaele, A. D. Rosa, N. Guignot, D. Andrault, J. E. F. S. Rodrigues, and G. Garbarino, Stability and equation of state of face-centered cubic and hexagonal close packed phases of argon under pressure, *Scientific Reports* **11**, 15192 (2021).

[19] B. L. Brugman, M. Lv, J. Liu, E. Greenberg, V. B. Prakapenka, D. Y. Popov, C. Park, and S. M. Dorfman, Strength, deformation, and the fcc–hcp phase transition in condensed Kr and Xe to the 100 GPa pressure range, *Journal of Applied Physics* **137**, 10.1063/5.0254842 (2025), publisher: AIP Publishing.

[20] M. Mezouar, G. Garbarino, S. Bauchau, W. Morgenroth, K. Martel, S. Petitdemange, P. Got, C. Clavel, A. Moyne, H.-P. Van Der Kleij, A. Pakhomova, B. Wehinger, M. Gerin, T. Poreba, L. Canet, A. Rosa, A. Forestier, G. Weck, F. Datchi, M. Wilke, S. Jahn, D. Andrault, L. Libon, L. Pennacchioni, G. Kovalskii, M. Herrmann, D. Laniel, and H. Bureau, The high flux nano-X-ray diffraction, fluorescence and imaging beamline ID27 for science under extreme conditions on the ESRF Extremely Brilliant Source, *High Pressure Research* **0**, 1 (2024), publisher: Taylor & Francis eprint: <https://doi.org/10.1080/08957959.2024.2363932>.

[21] A. Dewaele, F. Datchi, P. Loubeyre, and M. Mezouar, High pressure-high temperature equations of state of neon and diamond, *Physical Review B* **77**, 094106 (2008).

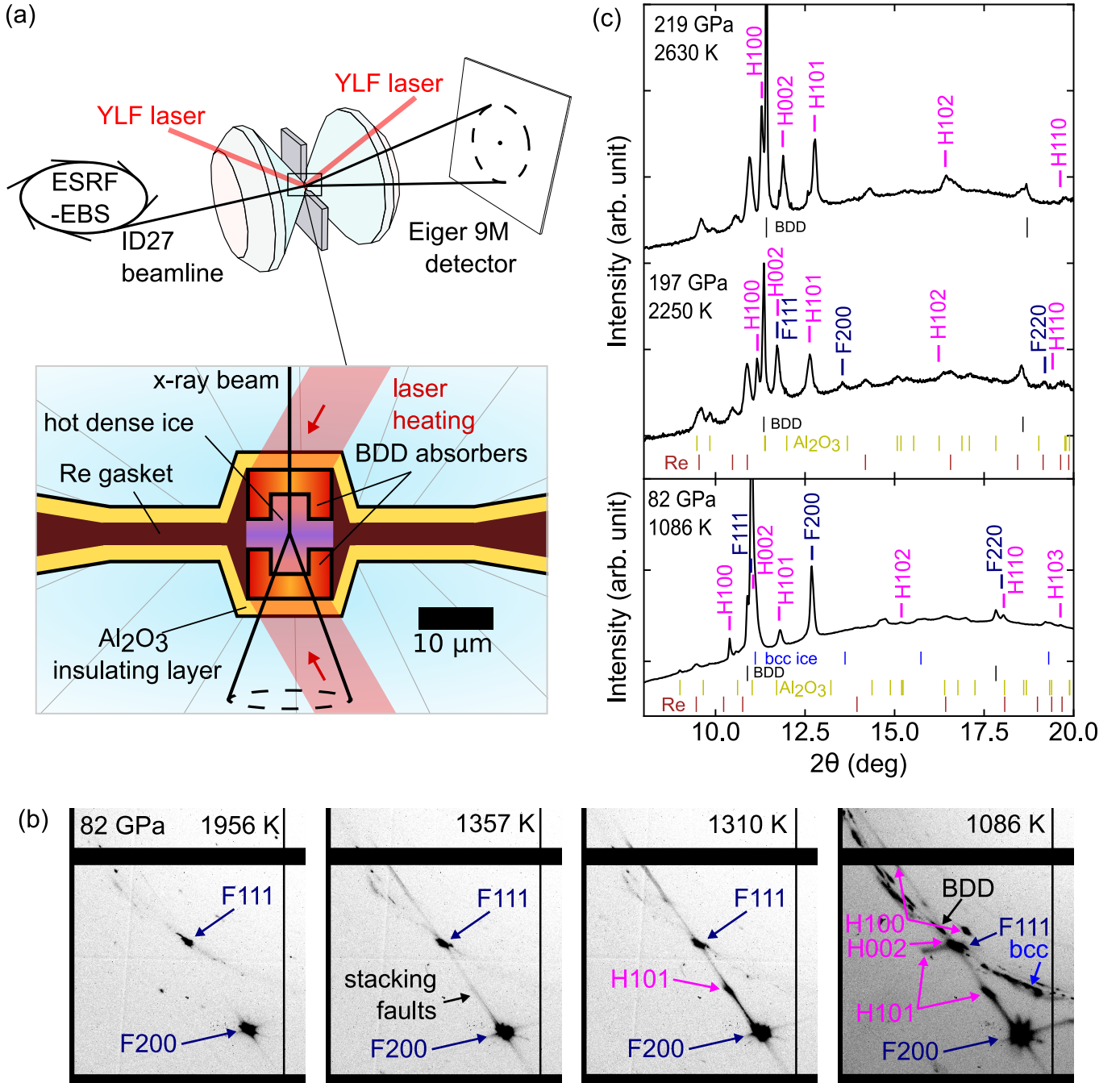


Figure 1. (a) Sketch of the sample assembly loaded in the DAC for XRD measurements on H_2O at extreme pressures and temperatures, scaled at around 200 GPa. (b) Series of diffraction images from run 1 on hot ice at 82 GPa, recorded while decreasing the temperature from 1986 K to 1086 K. The sequence illustrates the evolution of the 111 and 200 fcc reflections (denoted F111 and F200), the onset of X-ray diffuse scattering associated with the development of stacking faults, and the subsequent appearance of hcp Bragg reflections (H100, H002, and H101) below 1310 K. The final image, collected at 1086 K, corresponds to the end of the temperature ramp, during which the cell was rotated by 20° during XRD acquisition. (c) Integrated diffraction patterns measured at 82 GPa, 1086 K (bottom), 197 GPa, 2250 K (middle) and 219 GPa, 2630 K (top). XRD peaks from ice crystals are labeled in pink (hcp) and blue (fcc). The measured diffraction also includes contributions from bcc ice, the Re gasket, Al_2O_3 insulating layers (corundum phase), and BDD heaters, indicated by ticks.